



State Key Laboratory of Numerical Modelling for Atmospheric Sciences
and Geophysical Fluid Dynamics(LASG)
Institute of Atmospheric Physics Chinese Academy of Sciences

PDEs on the Sphere, 2014

Boulder, CO, USA

Solutions of 3-D Coordinate Surfaces of an Orthogonal Terrain-Following Coordinate and its Preliminary 2-D Advection Experiments

Jinxi Li¹, Yiyuan Li¹, Bin Wang^{1,2}

1 State Key Laboratory of Numerical Modeling for Atmospheric Sciences and Geophysical Fluid Dynamics,
Institute of Atmospheric Physics, Chinese Academy of Sciences, Beijing, China, 100029

2 Ministry of Education Key Laboratory for Earth System Modeling, and Center for Earth System Science,
Tsinghua University, Beijing, China, 100084

2014.4.7



Outline

- **Background**
- **Solutions of 3-D Coordinate Surfaces of an Orthogonal Terrain-Following Coordinate**
- **2-D Advection Experiments**
- **Conclusions**





A. Background





A.1 Importance of the numerical model

Atmospheric model

- **Weather forecast**
- **Climate simulation**
- ...

Dynamical core

- **One of the most important parts of an atmospheric model**
- **Prediction of wind, pressure and so on**
- ...

Vertical coordinate

- **An essential part of dynamical core**
- **Choice of vertical coordinate is the most important aspect of designing a model**
- ...

A- Background



A.2 The development of vertical coordinate

Z coordinate – Richardson (1922)

intuitive in the real space

P coordinate - Sutcliffe and Godart (1947)

continuous equation → diagnostic equation

Θ coordinate - Shapiro et al. (1973)

eliminate the computational errors of vertical motion

**Coordinate plane intersects with the terrain → initialize the grid above the terrain
→ computational errors**



Terrain-following σ coordinate

Low boundary → coordinate surface

- Phillips (1957); Gal-Chen and Somerville (1975)

Computational errors of pressure gradient and advection

A- Background



A.3 The problems of sigma coordinate

Pressure gradient error

- Interpolation method

Advection error

- Hybrid σ -coordinate

Non-orthogonal vertical grid

- Non-orthogonal transformation

Our research:

✧ 3-D solutions of coordinate surfaces of OS-coordinate

✧ Compare the OS-coordinate with the hybrid σ -coordinate

2005

- Transformation method
- Li et al., 2012

- Orthogonal sigma coordinate (OS-coordinate)
- Li et al., 2013

- Following coordinate in 2-D
- Sharman et al., 1988



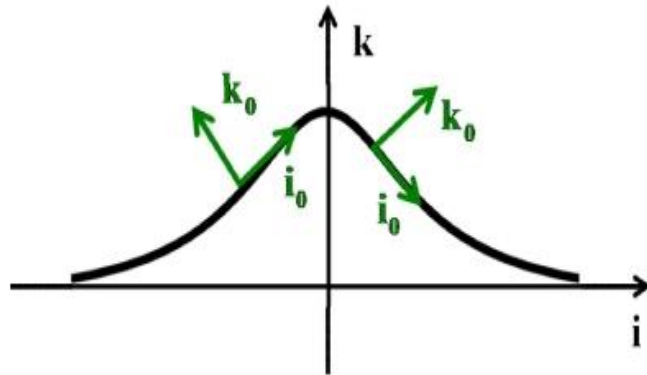
B.

Solutions of 3-D Coordinate Surfaces of an Orthogonal Terrain-Following Coordinate





B.0 Design of an orthogonal terrain-following coordinate



$$\begin{aligned}
 i_0 &= \cos b\lambda \cdot i - \sin b\theta \sin b\lambda \cdot j - \cos b\theta \sin b\lambda \cdot k \\
 j_0 &= \cos b\theta \cdot j - \sin b\theta \cdot k \\
 k_0 &= \sin b\lambda \cdot i + \sin b\theta \cos b\lambda \cdot j + \cos b\theta \cos b\lambda \cdot k
 \end{aligned}$$

2-D schematic of the coordinate rotation

Basis vectors in OS-coordinate

Equations of each three coordinate surface:

$$\begin{cases}
 \frac{\partial x'}{\partial x} = \cos b\lambda \\
 \frac{\partial x'}{\partial y} = -\sin b\theta \sin b\lambda \\
 \frac{\partial x'}{\partial z} = -\cos b\theta \sin b\lambda
 \end{cases}$$

$$\begin{cases}
 \frac{\partial y'}{\partial x} = 0 \\
 \frac{\partial y'}{\partial y} = \cos b\theta \\
 \frac{\partial y'}{\partial z} = -\sin b\theta
 \end{cases}$$

$$\begin{cases}
 \frac{\partial \sigma}{\partial x} = \sin b\lambda \\
 \frac{\partial \sigma}{\partial y} = \sin b\theta \cos b\lambda \\
 \frac{\partial \sigma}{\partial z} = \cos b\theta \cos b\lambda
 \end{cases}$$

$$\cos \theta = \frac{1}{\sqrt{1+H_y^2}}, \cos \lambda = \frac{\sqrt{1+H_y^2}}{\sqrt{1+H_x^2+H_y^2}}, \cos \theta' = \frac{1}{\sqrt{1+H_x^2}}, \cos \lambda' = \frac{\sqrt{1+H_x^2}}{\sqrt{1+H_x^2+H_y^2}}$$

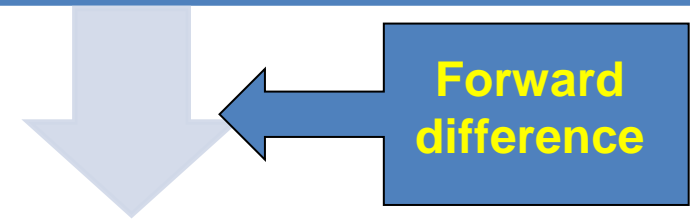
B- Solutions of 3-D Coordinate Surfaces of OS-coordinate



B.1 Idea of solving 3-D coordinate surfaces

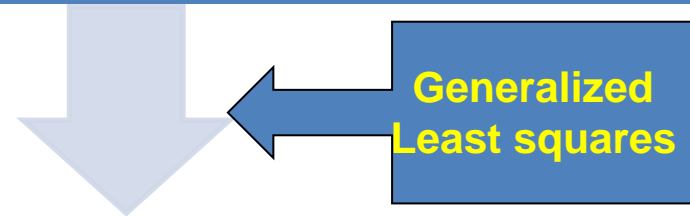
$$\begin{cases} \frac{\partial \sigma}{\partial x} = \sin b\lambda \\ \frac{\partial \sigma}{\partial y} = \sin b\theta \cos b\lambda \\ \frac{\partial \sigma}{\partial z} = \cos b\theta \cos b\lambda \end{cases}$$

1. Construct the partial differential equations (PDEs) of each coordinate surfaces



Forward
difference

2. Discrete the previous PDEs to obtain the linear algebraic equations (LAEs)

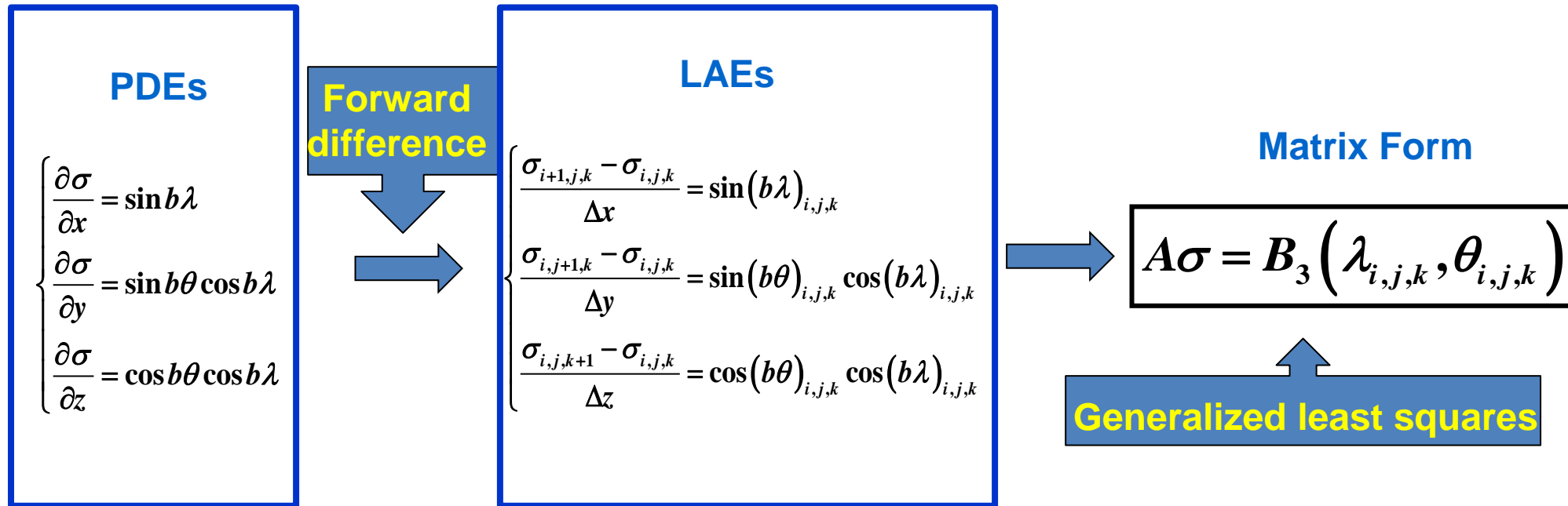


Generalized
Least squares

3. Obtain the numerical solutions of LAEs, which is exactly the coordinate surfaces



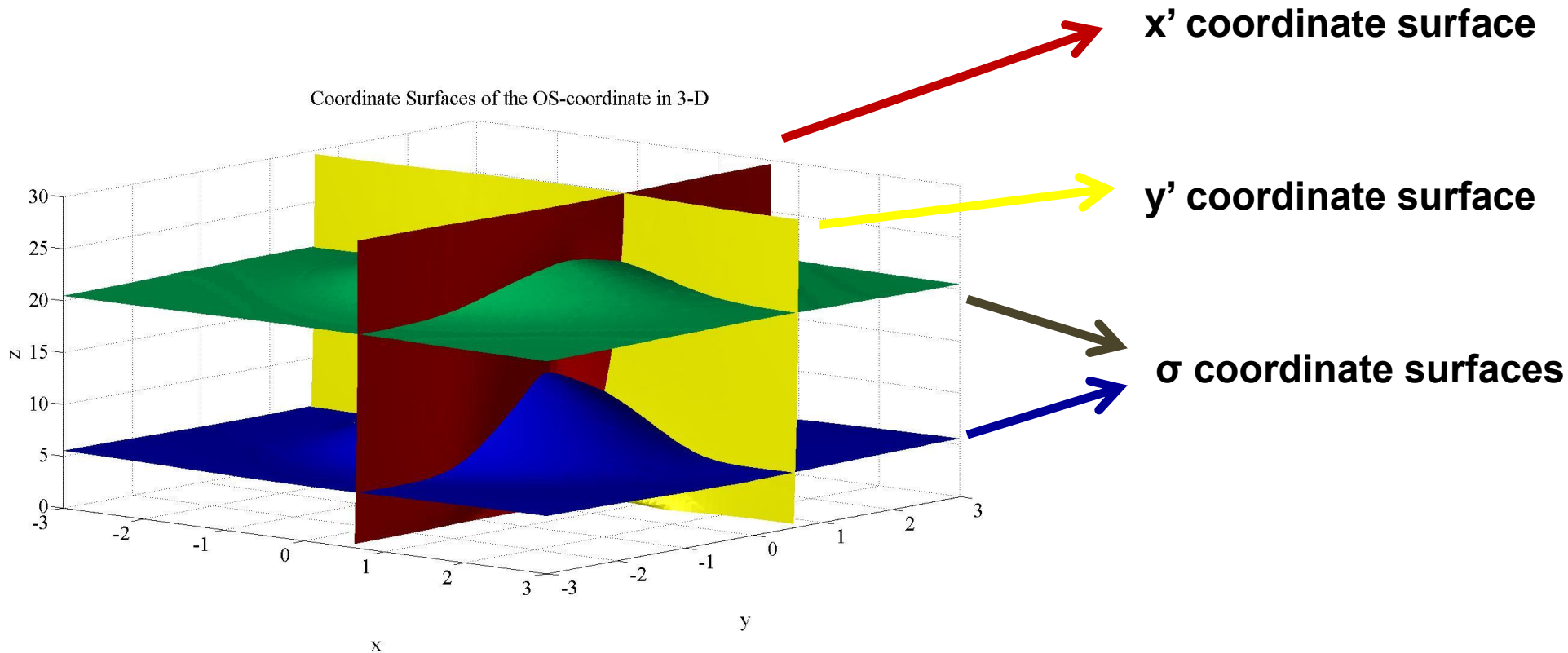
B.2 An example of solving the sigma coordinate surface



$$\sin \theta = \frac{H_y}{\sqrt{1 + H_y^2}}, \sin \lambda = \frac{H_x}{\sqrt{1 + H_x^2 + H_y^2}}$$



B.3 Coordinate surfaces of the OS-coordinate in 3-D

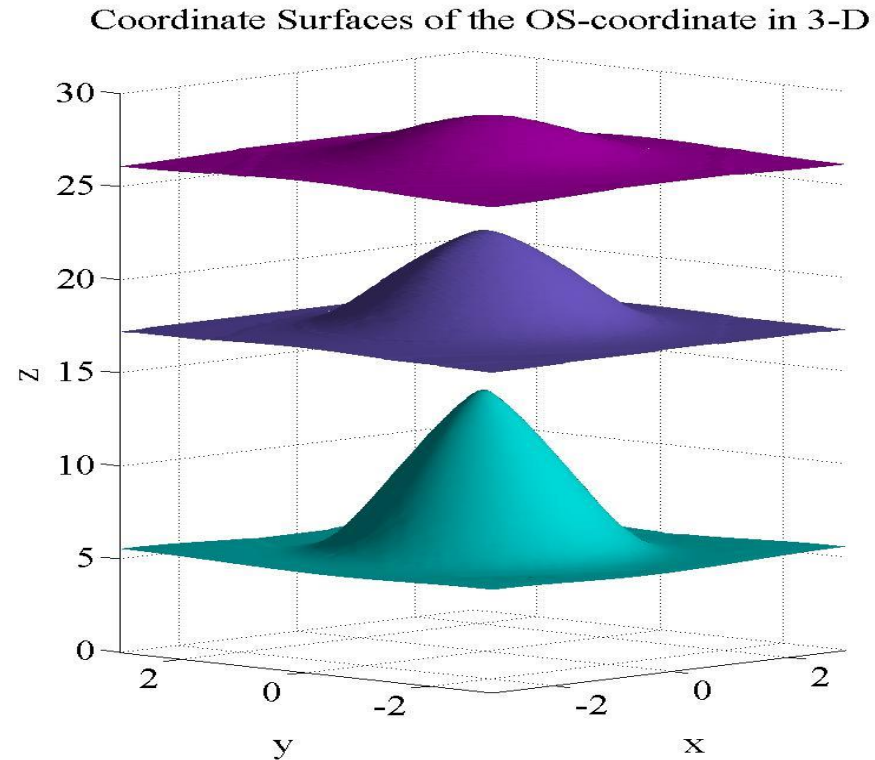


Conclusion:

1. Each two coordinate surfaces intersect orthogonally;
2. Intersection lines between every two coordinate surfaces **are curves** instead of lines.



B.4 Vertical variation of the σ -levels in the OS-coordinate



Conclusion:

Preserve the **benefits** of classic sigma coordinate

- Bottom σ -level coincides with the terrain
- Top σ -level becomes flat at the top of the model
- Slopes of the σ -levels decrease with increasing height

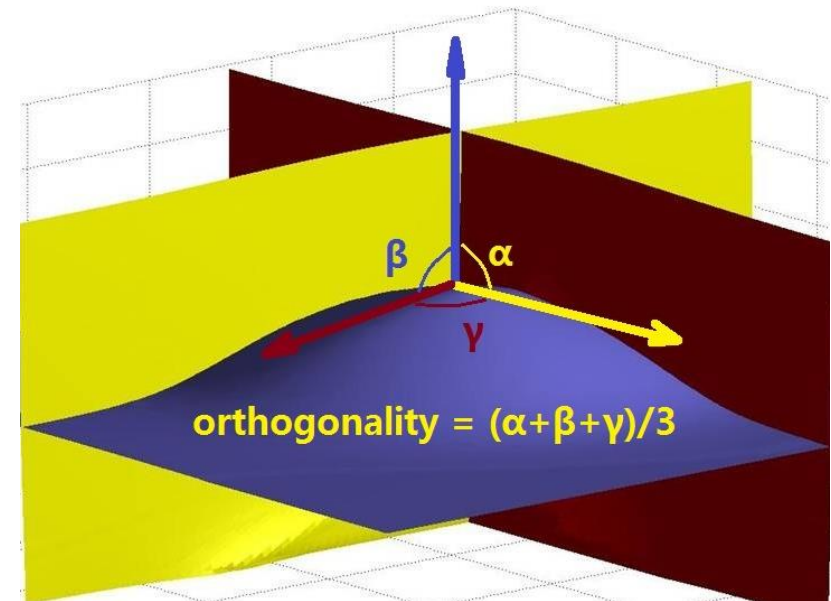


B.5 The orthogonality of 3-D numerical solutions of coordinate surfaces

Obtain the normal vectors of each coordinate surface via every grid point

Calculate the intersection angle between each two normal vectors

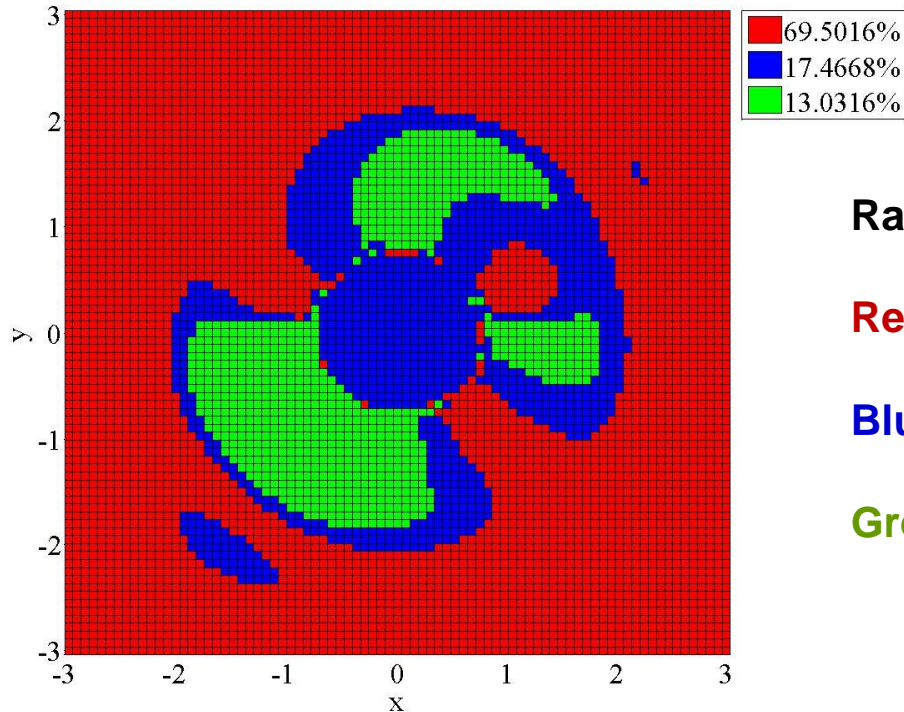
Calculate the orthogonality using those intersection angles





B.6 The orthogonality of the points on the coordinate surfaces of the OS-coordinate at the same height

The Orthogonality of the 3-D Coordinate Surfaces of the OS-coordinate



Range of angle in different colors:

Red: 80-100°

Blue: 70-80° or 100-110°

Green: 60-70° or 110-120°

Conclusion:

- 70%** of all the points on a coordinate surfaces is quasi-orthogonal.
- The **most non-orthogonal angles** appear above the **steepest** terrain.



B.7 A summary in short

We can do it

- Solve out the solutions of every coordinate surfaces in OS-coordinate in 3-D

But it is not good enough now

- Only 70% of points is nearly orthogonal at present
- Most non-orthogonal angles appear above the steepest terrain

However it can be improved

- Modify the PDEs of each coordinate surface
- Use other discretization method to obtain the LAEs
- Use high-order methods to solve the LAEs



C.

2-D Advection Experiments



C- 2-D Advection Experiments



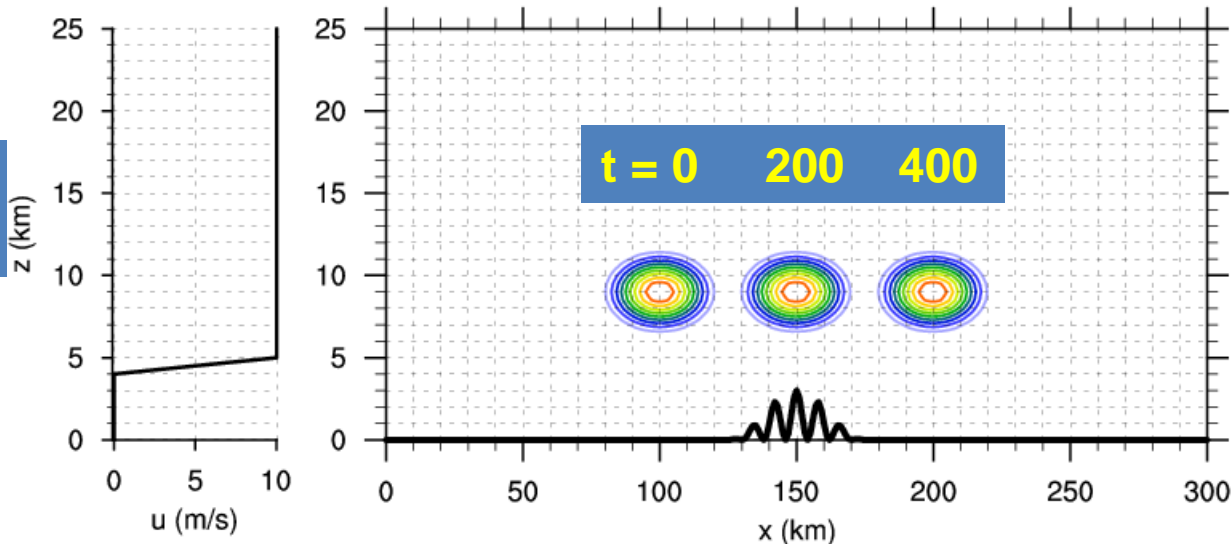
C.1 Schar-type 2-D linear advection experiments

(reproduce the experiments designed by Schär et al., 2002)

- OS-coordinate VS the corresponding hybrid σ -coordinate
- Wavelike terrain

$$\frac{q_{i,k}^{n+1} - q_{i,k}^{n-1}}{2\Delta t} + u \cdot \frac{q_{i+1,k}^n - q_{i-1,k}^n}{2\Delta X} + w \cdot \frac{q_{i,k+1}^n - q_{i,k-1}^n}{2\Delta Z} = 0$$

Horizontal
wind u



Analytical
solution

The colored contours in the right panel represent the tracer q with the contour interval of 0.1, and the thick black curve, the wavelike terrain.

C- 2-D Advection Experiments



C.2 Computational mesh in OS-coordinate and corresponding hybrid σ -coordinate

Two sets of comparable experiments:
(*similar slopes* of vertical layers in the same row)

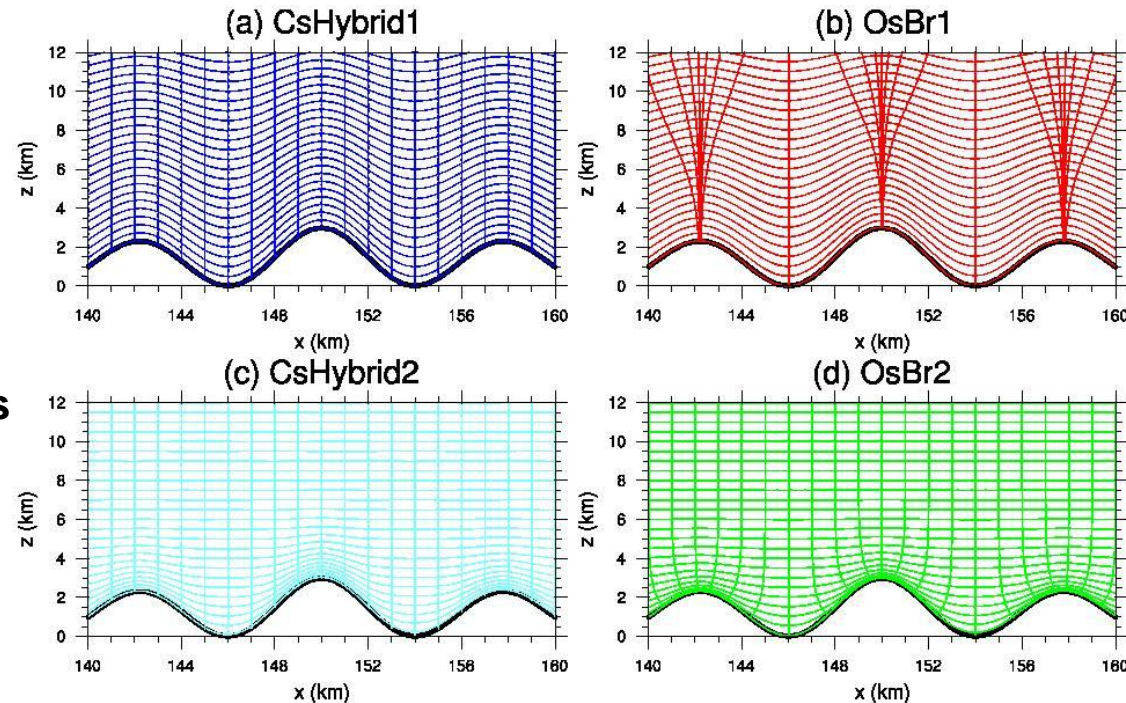
First row: steep slope of vertical layers

CsHybrid1, **OsBr1**

Second row: smooth slope of vertical layers

CsHybrid2, **OsBr2**

Computational Mesh in the Hybrid Sigma-Coordinate and the OS-coordinate



Comparison followed the three aspects:

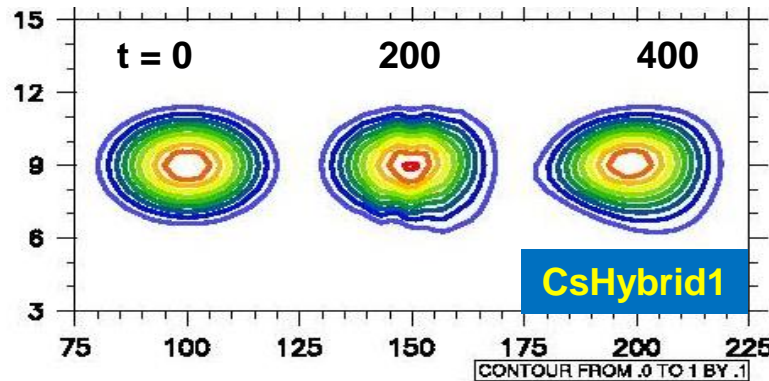
- The numerical solutions
- Root mean square errors (RMSEs)
- RMSEs reduction by the OS-coordinate

C- 2-D Advection Experiments

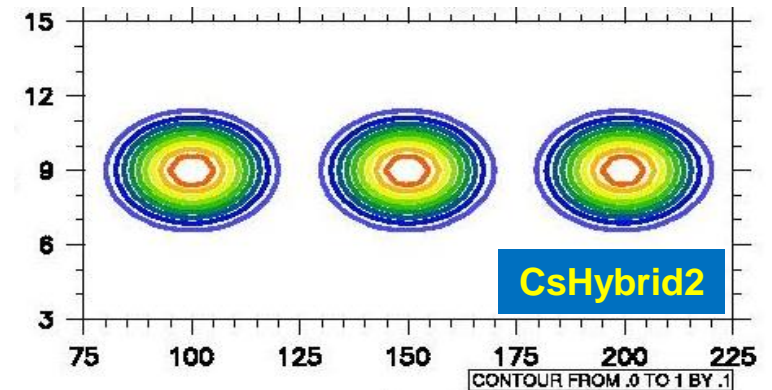


C.3 Numerical Solutions at three times

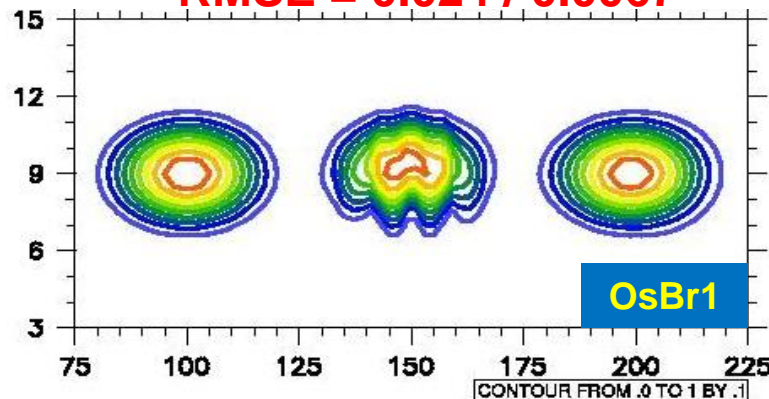
RMSE = 0.035 / 0.0097



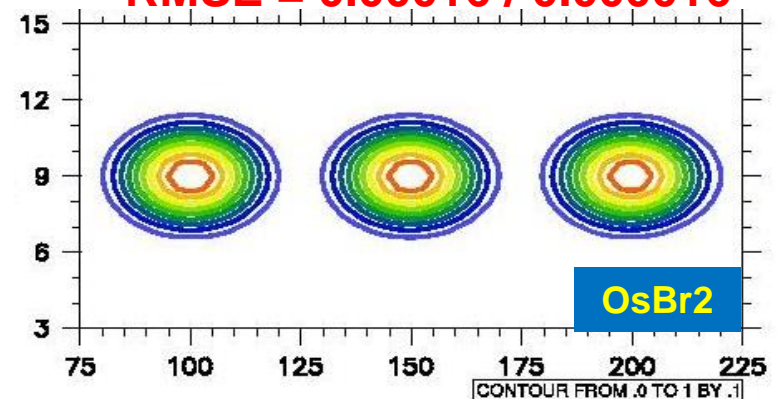
RMSE = 0.00023 / 0.000032



RMSE = 0.024 / 0.0067



RMSE = 0.00016 / 0.000016



Conclusion:

1. RMSE in OS-coordinate is **smaller** than that in corresponding hybrid σ -coordinate
2. **At the end** of the advection, the shape of the tracer in CsHybrid1 still has a **large deformation**; the shape of the tracer in OsBr1 is almost **recovered**.

Colored contours are the tracer q , with the contour interval of 0.1.

C- 2-D Advection Experiments

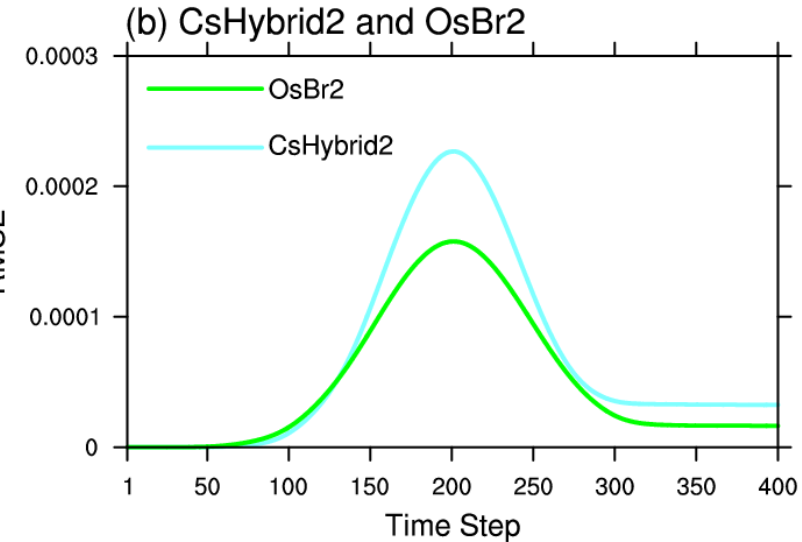
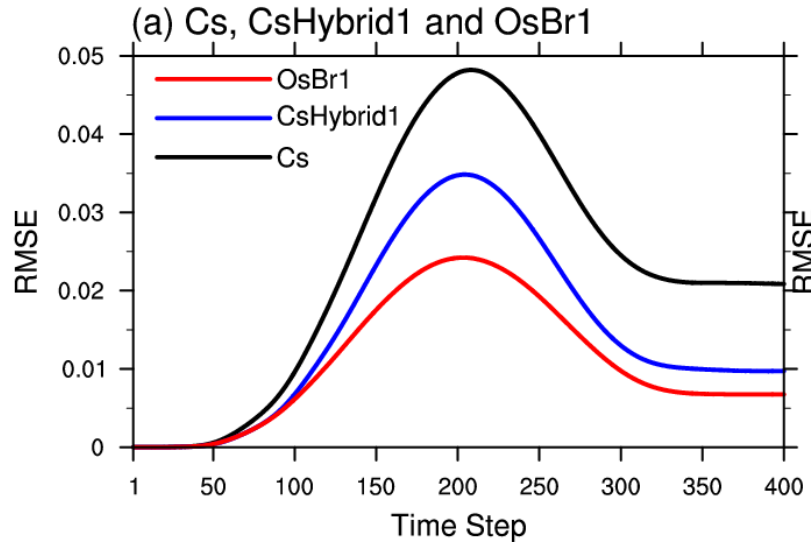


C.4 RMSEs of all five coordinates

Black :
Classic σ -coordinate

Blue and sky-blue :
hybrid σ -coordinate

Red and green :
OS-coordinate



Conclusion:

The RMSEs in the OS-coordinate is **much smaller** compared with the corresponding hybrid σ -coordinate.

C- 2-D Advection Experiments



C.5 RMSEs reduction by the OS-coordinate

Experiments	RMSEs		RMSEs reduction by the OS-coordinate	
	average	maximum	average	maximum
CsHybrid1	0.015	0.035	26.9%	30.5%
OsBr1	0.011	0.024		
CsHybrid2	0.000068	0.00023	25.5%	30.4%
OsBr2	0.000051	0.00016		



C.6 A summary in short

	Conclusion (compared with the corresponding hybrid σ -coordinate)
Numerical solutions	The shape of the tracer in OS-coordinate can be preserved at the end of the advection
RMSE	Much smaller in OS-coordinate



D. Conclusion



D- Conclusion



D.1 Solutions of 3-D coordinate surfaces of OS-coordinate

We can do it

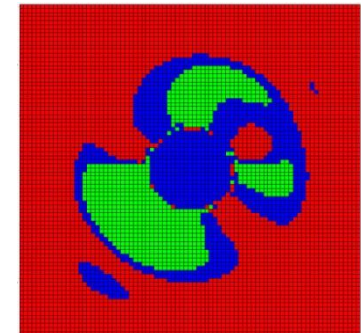
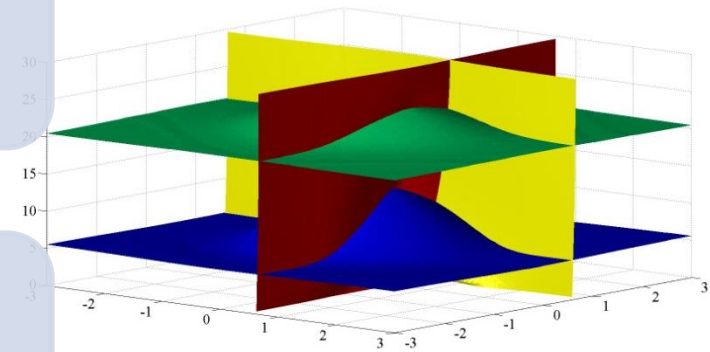
- Solve out the solutions of coordinate surfaces in OS-coordinate in 3-D

But it's not good enough now

- Only 70% of points is nearly orthogonal at present
- Most non-orthogonal angles are above the steepest terrain

However it can be improved

- Modify the PDEs
- Use other discretization method to obtain the LAEs
- Use high-order method to solve the LAEs





D.2 2-D advection experiments

1. The RMSEs in the OS-coordinate are much smaller than those of the corresponding hybrid σ -coordinate. The RMSEs reduction of the advection errors by the OS-coordinate is over 25% more.
2. The OS-coordinate can preserve the shape of the tracer much better than the hybrid σ -coordinate at the end of the advection.

Thank you!



LASG

THANKS

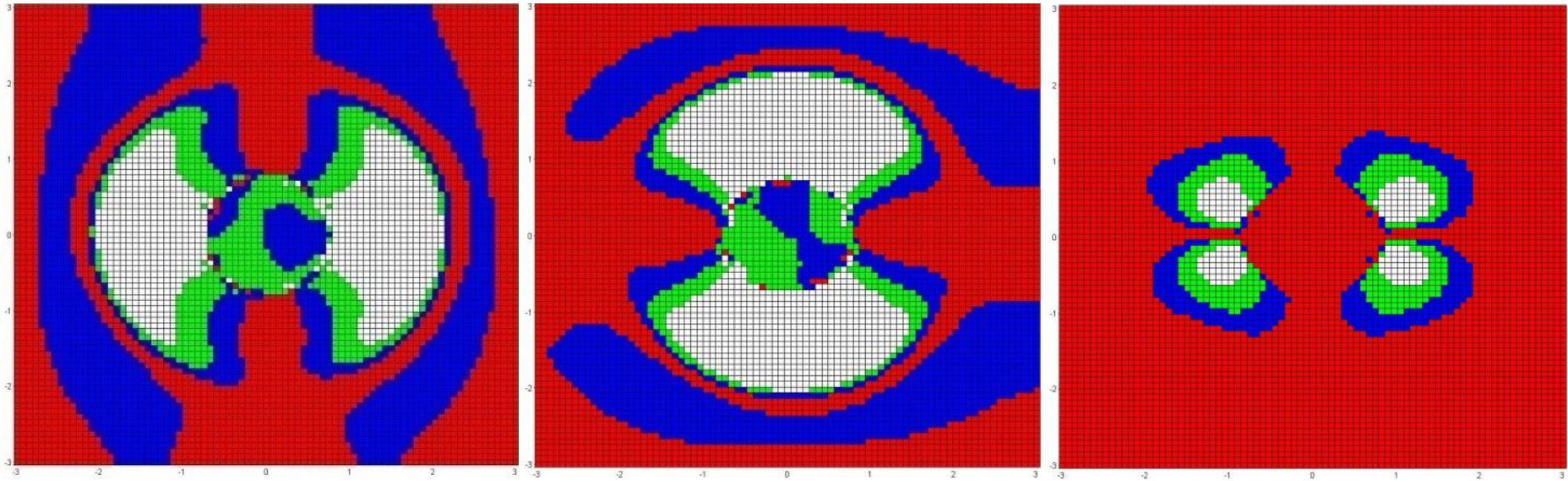


The logo features the word "LASO" in a bold, white, sans-serif font. The letter "O" is replaced by a circular emblem with green and yellow wavy lines and the text "LASG" inside. The background is a blue globe with a map of China, and the bottom of the image has an orange gradient.

LASO

THANKS

B.4 Result of angles between every two coordinate surface



α (x' & sigma)

β (y' & sigma)

γ (x' & y')

The orthogonality of the points on the coordinate surfaces of the OS-coordinate at a constant height.

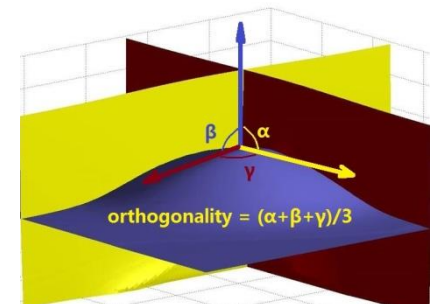
Range of angle in different colors:

Red: 80-100°

Green: 60-70° or 110-120°

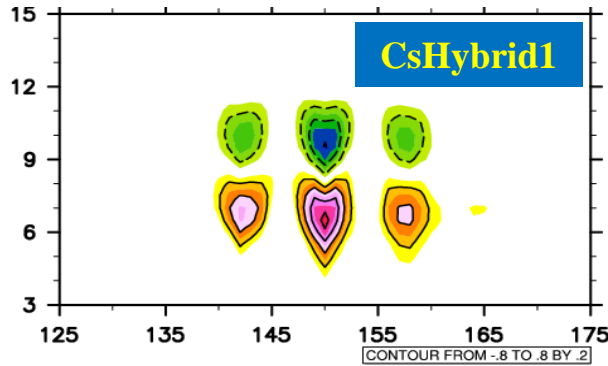
Blue: 70-80° or 100-110°

White: other angles

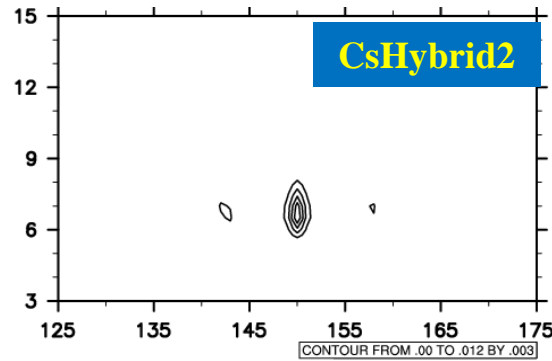


C.4 Absolute errors in the Schär-type experiments

Max = 0.871267

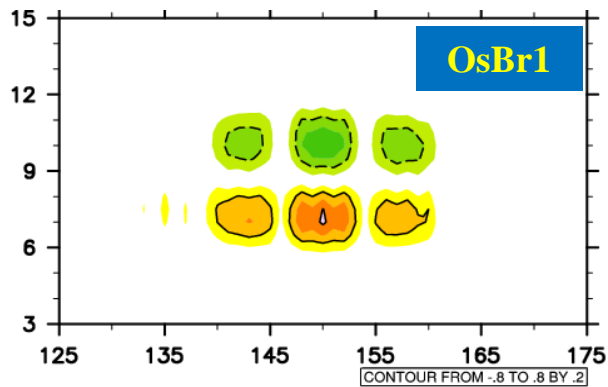


Max = 0.0152769

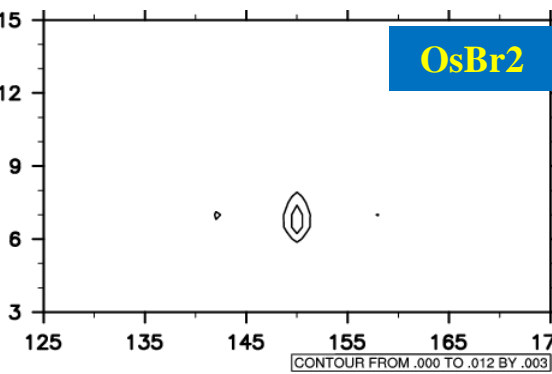


Absolute errors with the non-terrain simulation at $t = 200$

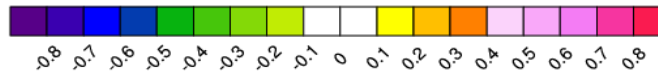
Max = 0.423437



Max = 0.00839093



The solid black contours are for positive values, and the dashed contours are for negative values. The contour interval is 0.2.



Conclusion:

1. The absolute errors in OS-coordinate are **much smaller** than those in the hybrid σ -coordinate.
2. The maximum absolute error in OsBr2 is two orders of magnitude less than those in OsBr1

Hybrid coordinate

OS coordinate



Further research

3D Solution

- **Obtain PDEs:** Seek the rotation angle of the vectors in the tangent plane
- **Obtain LAEs:** Change the difference methods
- **Numerical Solutions:** Change the numerical methods (generalized least square and conjugated gradient method)

Orthogonal Grid

- **Investigation**
- **Analysis of mechanism**



A.2 The development of vertical coordinate

Z coordinate-Richardson(1922)

P coordinate-Sutcliffe and Godart(1947)

Θ coordinate-Shapiro et al.(1973)

intuitive in the real space

continuous equation \rightarrow diagnostic equation

eliminate the computational errors of vertical advection

Coordinate plane intersects with the terrain \rightarrow initialize the grid above the terrain \rightarrow calculation errors



Terrain-following σ coordinate

- Phillips(1957);Gal-Chen and Sommerville(1975)

Low boundary \rightarrow coordinate surface

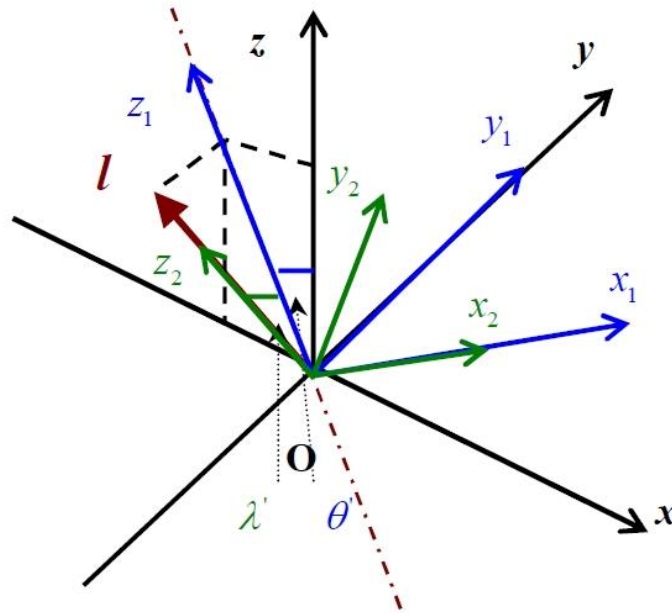
Computational errors of pressure gradient force and advection

η coordinate

- Mesinger(1984); Yu R. and Xu Y.,(2004)

Quasi-horizontal vertical coordinate surface

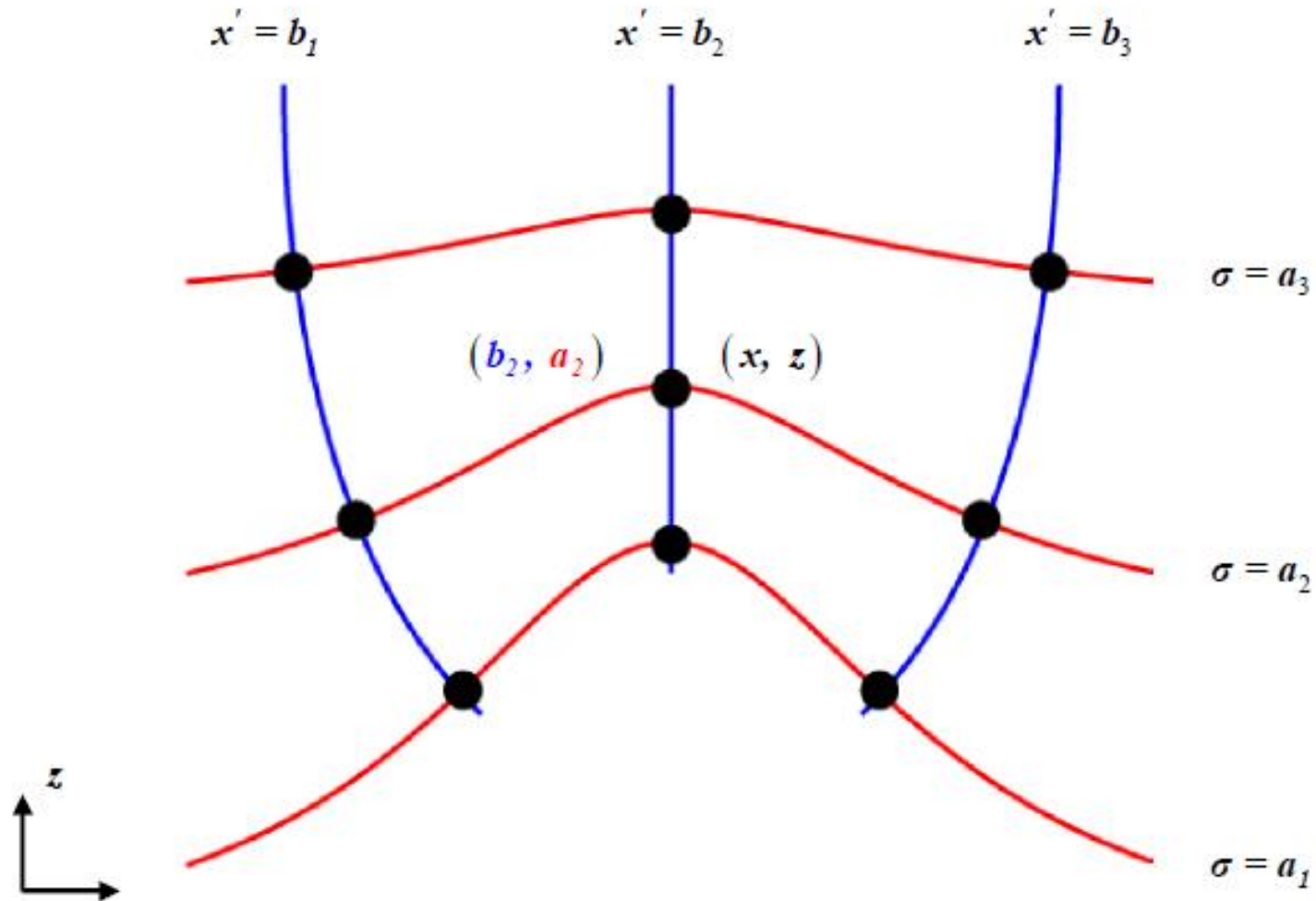
Rotation of OS-coordinate



3-D schematic rotation for solving the basis of the OS-coordinate on the upslope of the terrain.

The burgundy arrow is the normal vector of the terrain, and the burgundy dashdotted line is its projection on the plane Oxz . The black arrows are the basis vectors of the z coordinate, the blue arrows are the basis vectors of the first rotated coordinate $[O;x_1,y_1,z_1]$, and the green arrows are the basis vectors of the second rotated coordinate $[O;x_2,y_2,z_2]$.

Cross-Point Method



Calculate intersection points from the top of the model through x' coordinate line

Expressions of basis of OS-coordinate:

<p>The first kind</p>	$\begin{cases} \vec{i}_o = \cos \theta' \vec{i} + \sin \theta' \vec{k} \\ \vec{j}_o = -\sin \theta' \sin \lambda' \vec{i} + \cos \lambda' \vec{j} + \cos \theta' \sin \lambda' \vec{k} \\ \vec{k}_o = -\sin \theta' \cos \lambda' \vec{i} - \sin \lambda' \vec{j} + \cos \theta' \cos \lambda' \vec{k} \end{cases}$
<p>The second kind</p>	$\begin{cases} \vec{i}_o = \cos \lambda \vec{i} - \sin \theta \sin \lambda \vec{j} - \cos \theta \sin \lambda \vec{k} \\ \vec{j}_o = \cos \theta \vec{j} - \sin \theta \vec{k} \\ \vec{k}_o = \sin \lambda \vec{i} + \sin \theta \cos \lambda \vec{j} + \cos \theta \cos \lambda \vec{k} \end{cases}$

where $\cos \theta = \frac{1}{\sqrt{1+H_y^2}}, \cos \theta' = \frac{1}{\sqrt{1+H_x^2}}, \cos \lambda = \frac{\sqrt{1+H_y^2}}{\sqrt{1+H_x^2+H_y^2}}, \cos \lambda' = \frac{\sqrt{1+H_x^2}}{\sqrt{1+H_x^2+H_y^2}}$

Schär-type experiments (2002)

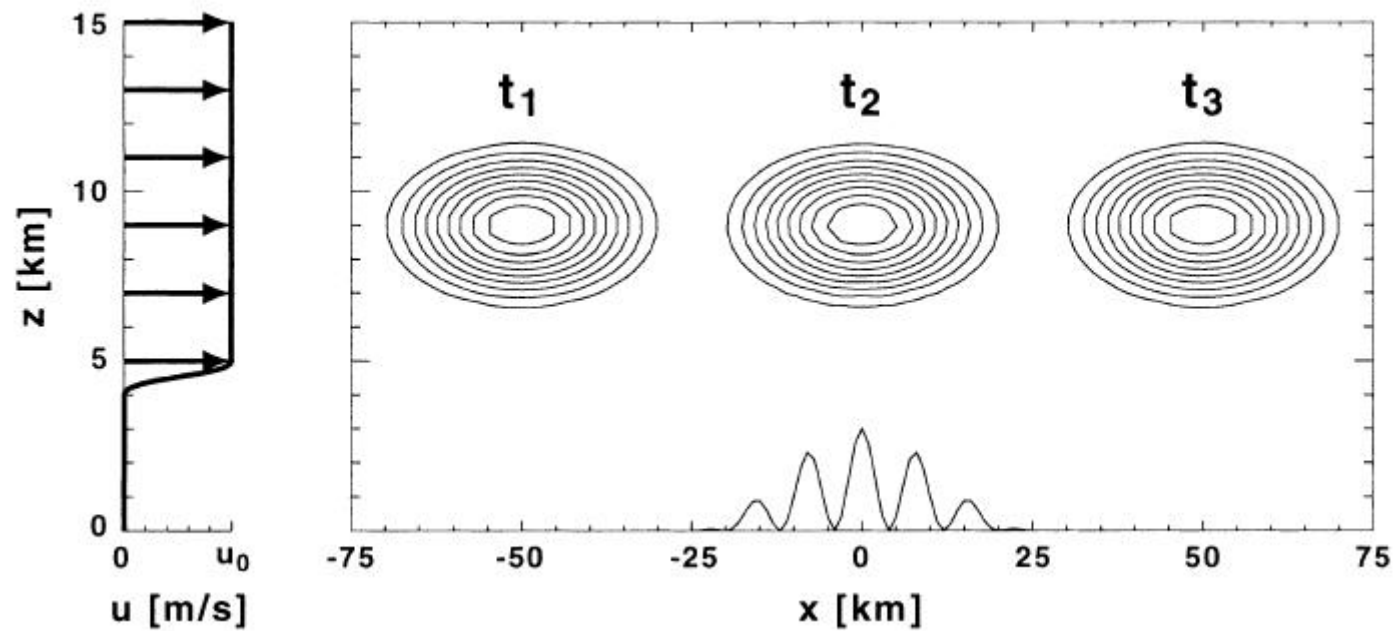
The new smooth level vertical **(SLEVE)** coordinate yields smooth coordinates at mid- and upper levels.

$$z(\sigma) = \sigma + h_1(x, y)b_1(\sigma) + h_2(x, y)b_2(\sigma)$$

$$b_i(\sigma) = \frac{sh \frac{H - \sigma}{s_i}}{sh \frac{H}{s_i}}$$

The basic concept of the new coordinate is to employ **a scale-dependent vertical decay s** of underlying terrain features.

Schär-type experiments (2002)

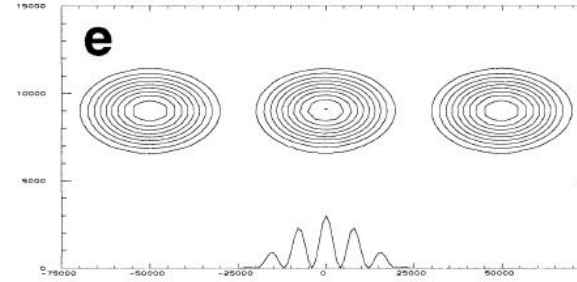
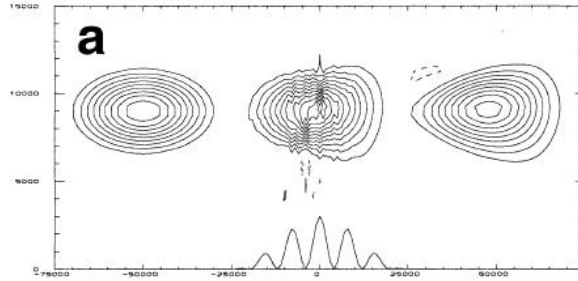


Vertical cross section of the idealized two-dimensional advection test.

The topography is located entirely within a stagnant pool of air, while there is a uniform horizontal velocity aloft. The analytical solution of the advected anomaly is shown at three instances.

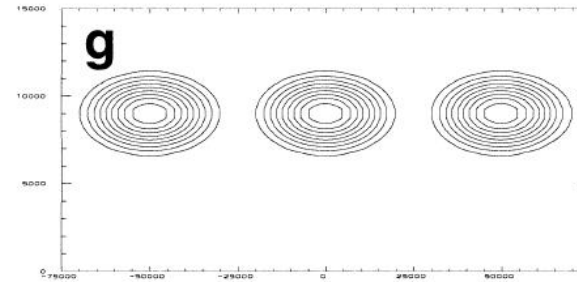
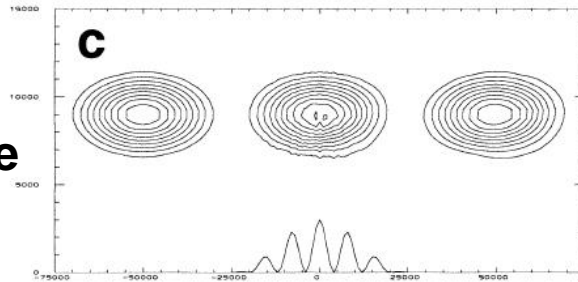
Schär-type experiments (2002)

σ coordinate



SLEVE coordinate

Hybrid coordinate



A regular grid

Numerical solutions to the advection test using centered differences and a horizontal Courant number of 0.25.

(a),(c),(e),(g) The advected anomalies at three consecutive times ($t_1 = 0$, $t_2 = 2500$ s, $t_3 = 5000$ s).

The initial amplitude of the anomaly is 1; the contour interval in the left-hand panels is 0.1, and that in the righthand panels is 0.01 (zero contour suppressed, negative contours dashed).

Parameters:

OS-coordinate VS the associated hybrid σ coordinate

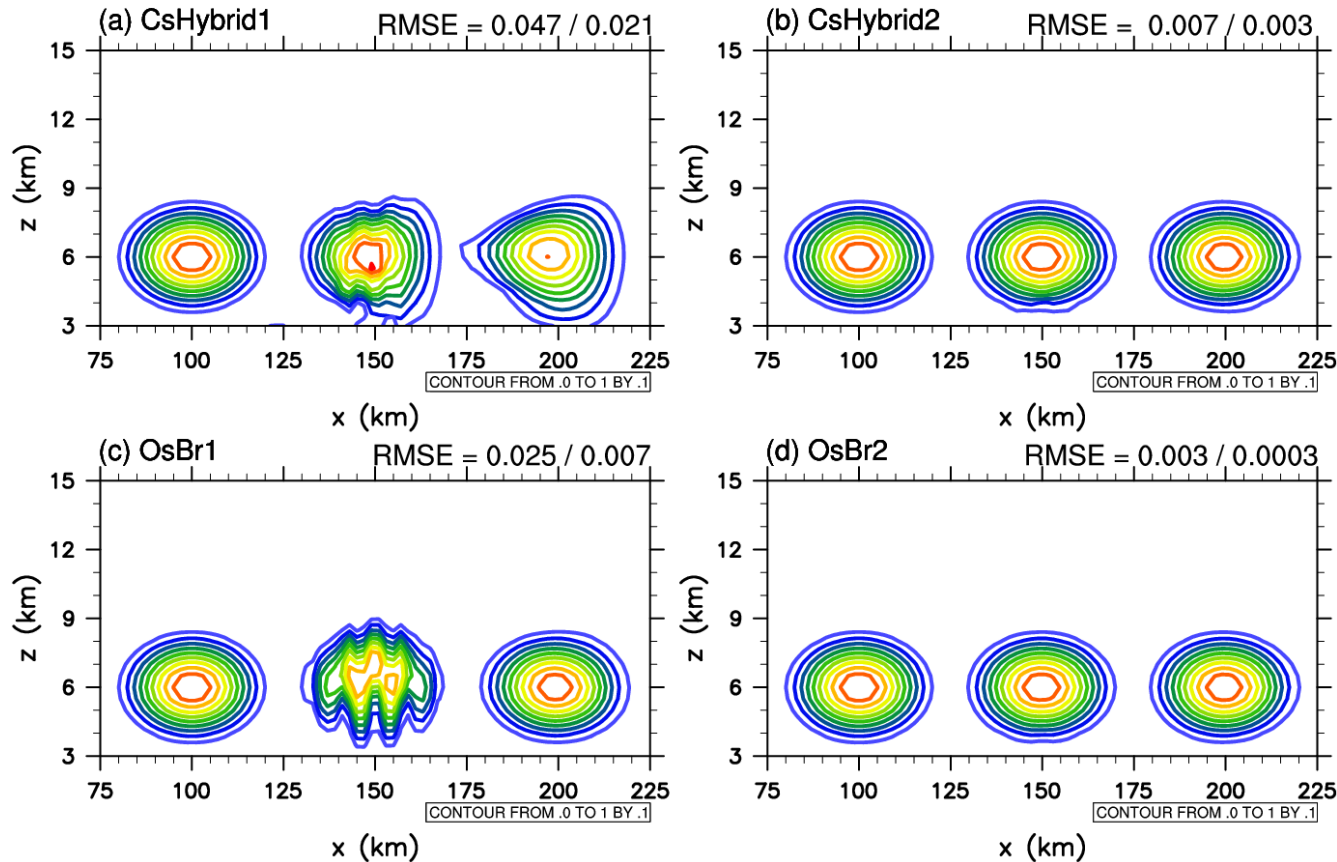
Wave-like terrain

To investigate

the distinct impact of the orthogonal grid of the OS-coordinate

Experiment parameters	Expressions
wave-like terrain	$h^*(x) = \begin{cases} h_0 \cos^2\left(\frac{\pi x}{2a}\right) & \text{for } x \leq a \\ 0 & \text{for } x \geq a \end{cases}$
	$h(x) = \cos^2\left(\frac{\pi x}{\lambda}\right) h^*(x)$
Experiment parameters	$b = \left(\frac{H_t - z}{H_t - h}\right)^n$
definition of hybrid σ coordinate	$\sigma = z - \left(\frac{H_t - z}{H_t - h}\right)^n \cdot h$
advection equation	$\frac{q_{i,k}^{n+1} - q_{i,k}^{n-1}}{2\Delta t} + u \cdot \frac{q_{i+1,k}^n - q_{i-1,k}^n}{2\Delta X} + w \cdot \frac{q_{i,k+1}^n - q_{i,k-1}^n}{2\Delta Z} = 0$
tracer	$q(x, z) = q_0 \cdot \begin{cases} \cos^2\left(\frac{\pi}{2} \cdot r\right), & r \leq 1 \\ 0 & \end{cases}$
u field	$u(z) = u_0 \cdot \begin{cases} 1 & , z_2 \leq z \\ \sin^2\left(\frac{\pi}{2} \cdot \frac{z - z_1}{z_2 - z_1}\right), & z_1 \leq z \leq z_2 \\ 0 & , z \leq z_1 \end{cases}$

Advection of Both Coordinates at Three Times in Low-Level Experiments



The advection at the beginning ($t = 0$), the middle ($t = 200$), and the end ($t = 400$) of the advection in the **modified Schär-type (low-level) experiments**.

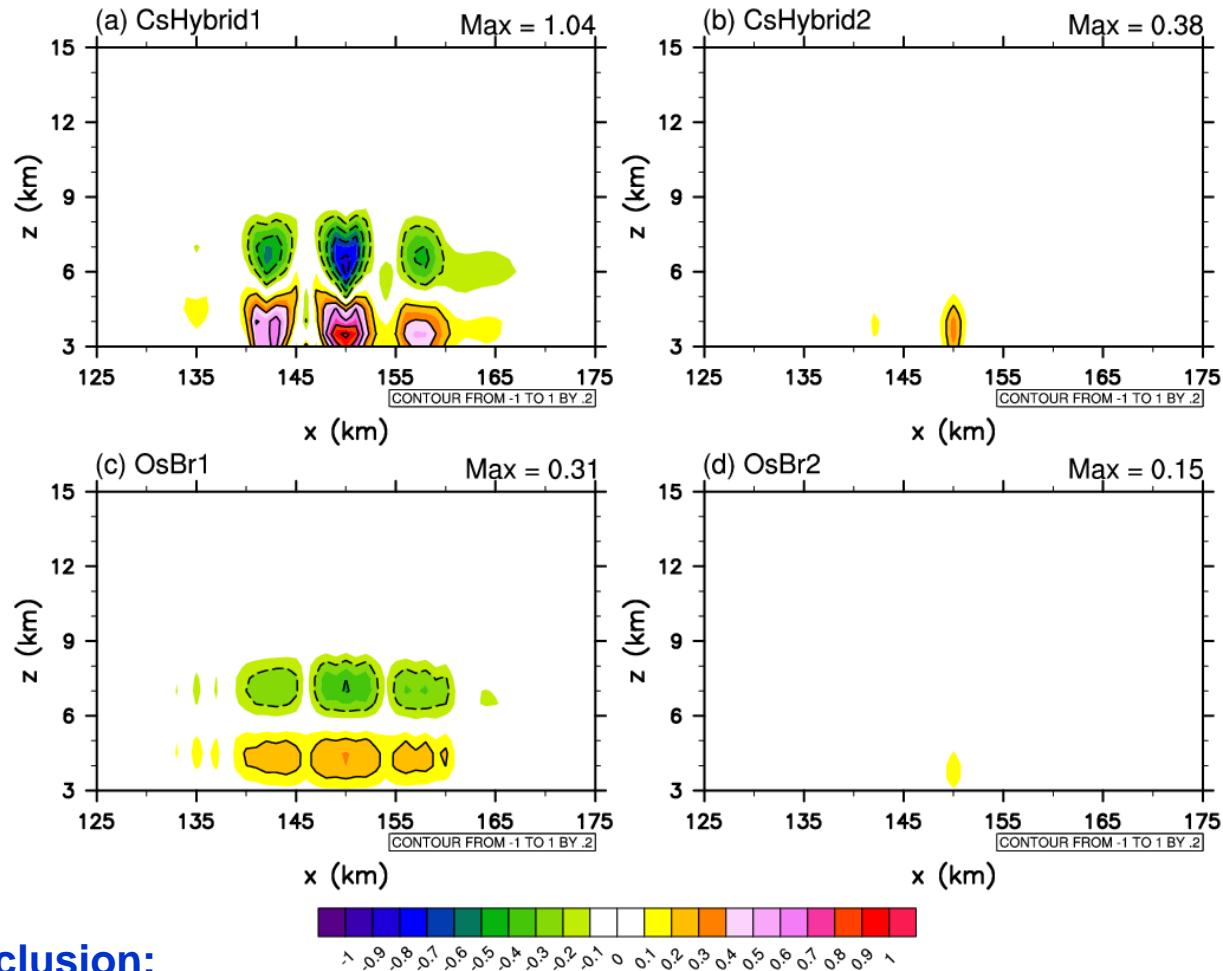
Colored contours are the tracer q , with the contour interval of 0.1.

Conclusion:

The slower the decay speed of rotation parameter is, the more apparent the deformation is.

When the advection is over the top of the terrain, there is large deformation with different kind in both CsHybrid1 and OsBr1. At the end of the advection, the shape of the tracer in CsHybrid1 still has a large deformation; however, the shape of the tracer in OsBr1 is almost recovered.

Absolute Errors of Both Coordinates in Low-Level Experiments



$t = 200$ s

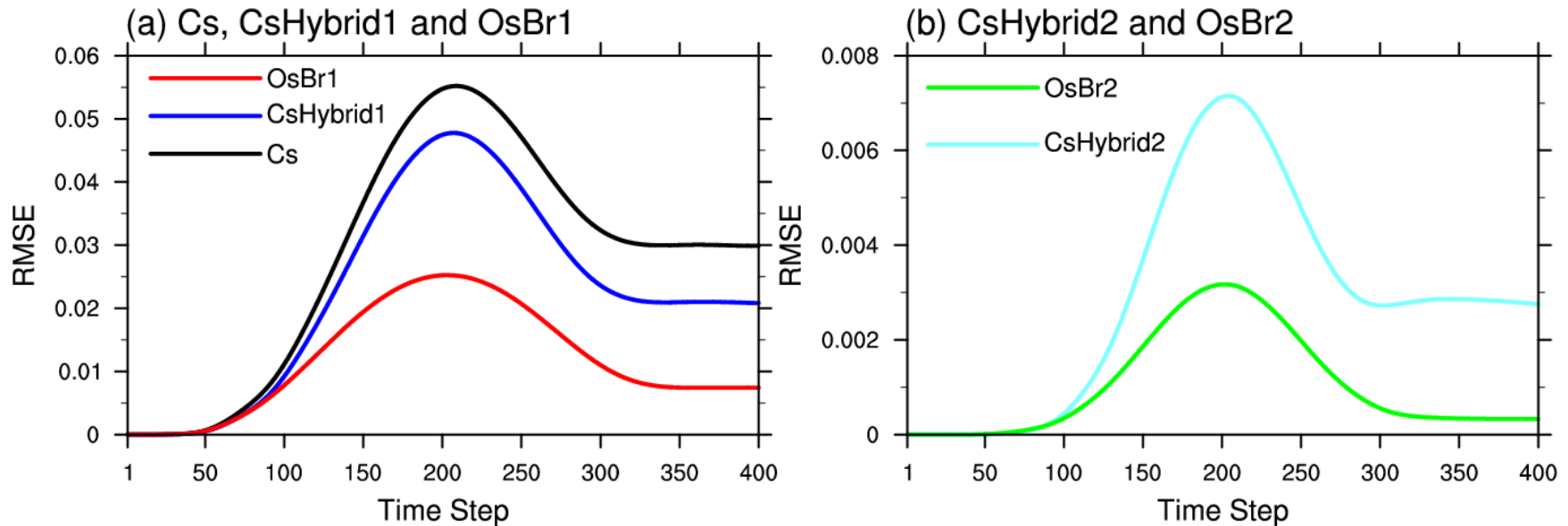
Absolute errors of the hybrid σ -coordinate and the OS-coordinate compared with **the non-terrain simulation**.

Shading represents the AE. The solid black contours are for positive values, and the dashed contours are for negative values. The contour interval is 0.2.

Conclusion:

The absolute errors in OS-coordinate are much smaller than those in the hybrid σ -coordinate.

RMSEs of All the Five Coordinates in the Low-Level Experiments



RMSEs of all five experiments with respect to **the non-terrain simulation** in the modified Schär-type (low-level) experiments at every time step.

Conclusion:

The RMSEs reduction of the advection errors by the OS-coordinate is about 50% more compared with the corresponding hybrid σ -coordinate.

**RMSE reduction by the OS-coordinate
in the Schär-type (high-level) experiments**

<i>Experiments</i>	<i>RMSEs</i>		<i>RMSEs reduction by the OS-coordinate</i>	
	<i>Unit: %</i>			
	average	maximum	average	maximum
CsHybrid1	0.015	0.035	26.9	30.5
OsBr1	0.011	0.024		
CsHybrid2	0.000068	0.00023	25.5	30.4
OsBr2	0.000051	0.00016		

**RMSE reduction by the OS-coordinate
in the modified Schär (low-level) experiments**

<i>Experiments</i>	<i>RMSEs</i>		<i>RMSEs reduction by the OS-coordinate</i>	
	<i>Unit: %</i>			
	average	maximum	average	maximum
CsHybrid1	0.029	0.048	47.5	47.2
OsBr1	0.0120	0.025		
CsHybrid2	0.0029	0.0072	63.5	55.7
OsBr2	0.0011	0.0032		